Inactivation of Lactobacillus leichmannii ribonucleotide reductase by F2CTP: adenosylcobalamin destruction and formation of a nucleotide based radical

Published in final edited form as:
Biochemistry. 2010 February 23; 49(7): 1396–1403. doi:10.1021/bi9021318.

Inactivation of *Lactobacillus leichmannii* ribonucleotide reductase by F_2CTP: adenosylcobalamin destruction and formation of a nucleotide based radical[§]

Gregory J. S. Lohman[‡], **Gary J. Gerfen**[¥], and **JoAnne Stubbe**[*,‡,†]

[‡]Department of Chemistry, Massachusetts Institute of Technology, Cambridge, MA 02139

[¥]Albert Einstein College of Medicine, Jack and Pearl Resnick Campus, 1300 Morris Park Avenue, Ullmann Building, Room 225, Bronx, NY 10461

[†]Department of Biology, Massachusetts Institute of Technology, Cambridge, MA 02139

Abstract

Ribonucleotide reductase (RNR, 76 kDa) from *Lactobacillus leichmannii* is a class II RNR that requires adenosylcobalamin (AdoCbl) as a cofactor. It catalyzes the conversion on nucleoside triphosphates to deoxynucleotides and is 100% inactivated by one equivalent (eq.) of 2′,2′-difluoro-2′-deoxycytidine 5′-triphosphate (F_2CTP) in <2 min. Sephadex G50 chromatography of the inactivation reaction for 2 min revealed that 0.47 eq. of a sugar moiety are covalently bound to RNR and 0.25 eq. of a cobalt III corrin are tightly associated, likely through a covalent interaction with C_{419} (Co-S) in the active site of RNR (Lohman et. al. (2009) *Biochemistry*, accompanying manuscript). After one hour, a similar experiment revealed 0.45 eq. of the Co-S adduct associated with the protein. Thus at least two pathways are associated with RNR inactivation: one associated with alkylation by the sugar of F_2CTP and the second with AdoCbl destruction. To determine the fate of [1′-^{3}H] F_2CTP in the latter pathway, the reaction mixture at 2 min was reduced with $NaBH_4$ (NaB^2H_4) and the protein separated from the small molecules using a centrifugation device. The small molecules were dephosphorylated and analyzed by HPLC to reveal 0.25 eq. of a stereo-isomer of cytidine, characterized by mass spectrometry and NMR spectroscopy, indicating the trapped nucleotide had lost both of its fluorides and gained an oxygen. High field ENDOR studies with [1′-^{2}H] F_2CTP from the reaction quenched at 30 s, revealed a radical that is nucleotide based. The relationship of this radical to the trapped cytidine analog provides insight into the non-alkylative pathway for RNR inactivation relative to the alkylative pathway.

Ribonucleotide reductases (RNRs) catalyze the conversion of nucleotides to deoxynucleotides providing the monomeric precursors required for DNA replication and repair.(1–5) Class I and Class II RNRs are stoichiometrically inactivated by the 5′-di and triphosphate forms of 2′-deoxy-2′,2′-difluorocytidine (Gemzar™, F_2C) a drug presently used clinically in the treatment of advanced pancreatic cancer and non small cell lung carcinoma.(6–11) The *Lactobacillus leichmannii* ribonucleoside triphosphate reductase, RTPR, a monomer of molecular weight 76 kDa, is the paradigm for adenosylcobalamin (AdoCbl) requiring RNRs, although recent

[§]Funding for this study was provided in part by NIH grant GM-29595.

*To whom correspondence should be addressed. Tel: (617) 253-1814, Fax: (617) 258-7247, stubbe@mit.edu.

SUPPORTING INFORMATION AVAILABLE

UV-vis spectra of cobalamin standards (Figure 1S) and small molecule fraction from Sephadex G50 chromatography of the inactivation experiment (Figure 2S). 130 GHz EPR spectra of RTPR with F_2CTP and [1′-^{2}H]-F_2CTP (Figure 3S). This material is available free of charge via the Internet at http://pubs.acs.org.

genomic analyses have revealed that the dimeric class II enzymes, exemplified by the recently crystallized *Thermotoga maritima* RTPR, are much more prevalent than the monomeric forms.(12–15) In the accompanying paper we reported the synthesis of [1′-^{3}H]-, [1′-^{2}H]-, and [5-^{3}H]-F_2CTP and showed that one equivalent (eq.) of [1′-^{3}H]-F_2CTP resulted in 90% inhibition of the enzyme within 30 seconds with 0.47 eq. of ^{3}H covalently attached to the enzyme.(16) Our earlier studies demonstrated that during this inactivation, on a 30 min time scale, that RTPR became covalently labeled with the corrin ring of AdoCbl through C_{419}, one of the active site cysteines providing reducing equivalents to generate dNTPs.(17) In the present paper we describe our efforts to examine the fate of AdoCbl immediately subsequent to enzyme inactivation and the fate of the remaining F_2CTP that is not covalently attached to the enzyme. As with many mechanism based inhibitors of RNRs, multiple modes of inhibition are observed.(1,18) A model to accommodate our observations described in this paper in relationship to the observations in the accompanying manuscript is presented (Scheme 1).

MATERIALS AND METHODS

Quantification and characterization of cobalamin, cytosine, and nucleotide products generated from RTPR inactivated by F_2CTP

The inactivation mixture in final volume of 1250 μL contained: pre-reduced RTPR (50 μM), dATP (500 μM), AdoCbl (50 μM), HEPES (25 mM, pH 7.5), EDTA (4 mM), and $MgCl_2$ (1 mM). After addition of AdoCbl, all aliquots were handled under red light and wrapped with foil. The inactivation was initiated by addition of either [1′-^{3}H]-F_2CTP (specific activity (SA) 1985 cpm/nmol) or [5-^{3}H]-F_2CTP (SA 1350 cpm/nmol) to a final concentration of 50 μM. An aliquot was assayed for activity as described in the accompanying paper.(16) The inactivation was allowed to proceed for either 2 min or 1 h at 37°C. An aliquot (100 μL) was removed after 2 min and after 1 h, quenched by filtration through a YM-30 membrane at 4°C, the nucleotides dephosphorylated with alkaline phosphatase and analyzed by HPLC. An aliquot of 1000 μL after 2 min and 1 h was loaded on a Sephadex G-50 column (1 × 20 cm, 20 mL) wrapped in foil, run at 4°C under dim red light. The column was equilibrated in and eluted with 25 mM HEPES pH 7.5, 4 mM EDTA, and 1 mM $MgCl_2$, and 1 mL fractions were collected. Each fraction was assayed for A_{260nm} and A_{280nm} , and for radioactivity (100 μL). Aliquots (750 μL) from the protein containing fractions were combined and the UV-vis spectrum recorded. These fractions were then lyophilized to dryness (excluding light). Aliquots (750 μL) from the small molecules fractions (pooled when $A_{260} > A_{280}$) were combined and lyophilized to dryness (excluding light). These samples were dissolved in 500 μL water, and the UV-vis spectra recorded. The spectrometer baseline was determined by lyophilizing an equal volume of buffer identical to that used in the experimental samples, which was redissolved in 500 μL of water. The visible spectra of protein-associated cobalamin products were quantified by comparison to a standard of glutathionine cobalamin (GSCbl).(19) The corrin species not associated with the protein were deconvoluted through linear combinations of the spectra of AdoCbl and HOCbl standards in proportions ranging from 1:0 AdoCbl:HOCbl to 0:1 AdoCbl:HOCbl in 0.05 eq. increments. The samples were scaled to match the A_{525nm} of the experimental sample, and subtracted.

Characterization of major nucleoside product(s) isolated from a $NaBH_4$ quenched RTPR/ F_2CTP inactivation mixture

The reaction mixture contained in a final volume of 2 mL: RTPR (125 μM), dATP (500 μM), AdoCbl (125 μM), F_2CTP (125 μM), HEPES (25 mM, pH 7.5), EDTA (4 mM), and $MgCl_2$ (1 mM). The inactivation mixture was quenched at 2 min with 500 μL of 250 mM $NaBH_4$ in 500 mM Tris pH 8.5 in a 4.0 mL falcon tube and incubated 5 min at 37°C. The $NaBH_4$ solution was prepared by combining solid $NaBH_4$ with the buffer immediately before use. Vigorous foaming occurred during the inactivation. The solution was then filtered through a YM-30

membrane for 15 min at 14,000 × g at 4°C, and the flow through was treated with 200 U alkaline phosphatase for 2 h at 37°C, followed by filtration through a second YM-30 membrane. The sample was acidified by addition of glacial acetic acid and the resulting mixture was lyophilized to dryness to hydrolyze borate esters. The residue was then taken up in 1 mL 10 mM NH_4OAc and purified on an Altech Adsorbosphere Nucleotide Nucleoside C-18 column (250 mm × 4.6 mm) using a 2 mL injection loop with elution at a flow rate of 1 mL/min The solvent system for elution was composed of Buffer A (10 mM NH_4OAc, pH 6.8) and Buffer B (100 % methanol). The products were eluted with 100 % A for 10 min followed by a linear gradient to 40% B over 25 min and then to 100 % B over 5 min. Under these conditions the standards eluted as follows (compound, retention time): cytosine, 5.7 min; uracil, 7.9 min; cytidine (C), 12.6 min; arabinocytidine (*ara*-C), 17.4 min; deoxycytidine (dC), 19.0 min; and F_2C, 23.2 min. Diode array detection of the eluent allowed identification of cytosine containing nucleosides between 17 min and 22 min. These fractions were pooled and the recovery of cytosine-containing nucleosides determined to be ~60 nmol based on A_{270nm}. This material was lyophilized to dryness, taken up in 1 mM NH_4OAc, and re-purified using the same elution program, substituting 1 mM NH_4OAc, pH 6.8, for buffer A and retaining buffer B (100% MeOH). The major cytosine-containing material eluted at 16.2 min and was collected (~35 nmol), lyophilized, and rechromatographed a third time. The final recovery of nucleoside was typically 8–12 nmol. NMR and ESI MS: ^{1}H-NMR (500 MHz, D_2O) δ: 7.71 (d, *J* = 7.5 Hz, 1H, H6), 5.99 (d, *J* = 6.1 Hz, 1H, H1′), 5.85 (d, *J* = 7.5 Hz, 1H, H5), 4.41 (dd, *J* = 5, 6 Hz, 1H, H2′), 4.24 (dd, *J* = 4.3 Hz, 4.9 Hz, 1H, H3′), 4.02 (m, 1H, H4′), 3.80 (dd, *J* = 4.0, 12 Hz, 1H, H5′), 3.75 (dd, *J* = 7.0, 12 Hz, 1H, H5″). ESI-MS ($C_9H_{13}N_3O_5$) *m/z* ($M + Na^+$) calcd 266.0747, obsd 266.0743; ($M + H^+$) calcd 244.0928, obsd 244.0921.

Characterization of major nucleoside product isolated from $NaBD_4$ quenched RTPR/F_2CTP inactivation mixture

A reaction was run identically to that described above, except that $NaBD_4$ was substituted for $NaBH_4$. The final recovery of the trapped nucleotide after three purifications was ~5–8 nmol. ^{1}H-NMR (500 MHz, D_2O) δ: 7.71 (d, *J* = 7.5 Hz, 1H, H6), 5.98 (s, 1H, H1′), 5.84 (d, *J* = 7.5 Hz, 1H, H5), 4.01 (dd, *J* = 4.0 Hz, 7.1 Hz, 1H, H4′), 3.80 (dd, *J* = 4.0, 12 Hz, 1H, H5′), 3.75 (dd, *J* = 7.0, 12 Hz, 1H, H5″).

High Frequency EPR/ENDOR spectroscopy

Samples for D-band (130 GHz) EPR analysis were prepared from a reaction mixture which contained in a final volume of 50 μL: RTPR (300 μM), dATP (1 mM), AdoCbl (450 μM), F_2CTP (unlabeled, [1′-^{2}H], or [3′-^{2}H]) (300 μM), TR (20 μM), TRR (0.5 μM), NADPH (1 mM), HEPES (25 mM, pH 7.5). The dATP and reductants were mixed, followed by addition of RTPR. The AdoCbl was then added and mixed in low light, and the inhibition was initiated by the addition of F_2CTP or [1′-^{2}H]-F_2CTP. The reaction mixture was drawn up into the D-band EPR sample tube (O.D. 0.55 mm, I.D. 0.4 mm) mounted in the plastic tip of a pipette-man and then quenched in isopentane cooled with liquid nitrogen. The reaction time was 30 s. The tubes were mounted in the D-band probe under liquid nitrogen and pulsed EPR/ENDOR spectra were obtained on a spectrometer described elsewhere(20,21) using parameters listed in the figure legend to Figure 4. The field for D-band EPR spectra was calibrated using Mn^{2+} doped in MgO.(22)

RESULTS

Fate of AdoCbl during the inactivation of RTPR by F_2CTP

To gain a better understanding of the partitioning between the inactivation mechanism associated with covalent modification by a sugar moiety derived from F_2CTP(16) and the one associated with covalent modification of C_{419} by the corrin, the fate of AdoCbl was

investigated. Inactivation studies were carried out with AdoCbl:RTPR:F_2CTP in a ratio of 1:1:1 and the protein and small molecules were separated by Sephadex G50 chromatography and analyzed at 2 min and at 1 h. The small molecules and protein were analyzed for corrin by UV-vis spectroscopy either before or subsequent to concentration. Despite the detection by stopped flow spectroscopic methods on the ms time scale of cob(II)alamin (0.7 eq. per RTPR) and by the rapid freeze-quench (RFQ) EPR method (1.4 radicals, cob(II)alamin exchange coupled to a thiyl radical), no cob(II)alamin was observed on the time scale of these experiments.(17)

For quantitation of cobalamin derivatives, the small molecule products were analyzed assuming a mixture of AdoCbl, HOCbl and other Co(III) species. Both AdoCbl and HOCbl have λ_{max} at 523 nm with $\varepsilon = 8000\ M^{-1}cm^{-1}$. The protein associated cobalamins were quantitated using GSCbl, λ_{max} at 525 nm with $\varepsilon = 8000\ M^{-1}cm^{-1}$, a model for C_{419} attached to the corrin. The spectral features associated with each of these standards are shown in Figure 1S (supporting information, SI) The UV-vis spectra of the small molecule products of the inactivation mixture, after concentration, are shown at 2 min and 1 h in Figure 1A and B, respectively. RTPR co-eluted with 0.24 ± 0.3 eq. (average of three experiments) of a cobalt III containing corrin at 2 min and 0.48 ± 0.03 eq. at 1 h. The amount of cob(III)alamin species remaining in solution was 0.65 ± 0.1 eq. and 0.45 ± 0.1 eq. at 2 min and 1 h, respectively. At the two min time point, the 0.47 eq. of sugar covalently attached to RTPR and the 0.24 eq. with tightly-bound corrin, account for the complete inactivation (0.69 eq.). We have shown in our previous presteady state studies that recombinant RTPR is only 70 to 80% active protein.(23–26) As described in more detail subsequently, the 0.24 eq. is close to the amount of F_2CTP derived nucleotide that has been trapped and characterized.

At both 2 min and 1 h, the protein bound species resembles GSCbl (compare Figure 1A with Figure 1B). More of this material is seen at 1 h, suggesting covalent modification of C_{419} is occurring on a slow time scale and continues after complete inactivation (2 min). The spectra of the small molecules are very different at the two time points. Analysis of the 1 h spectrum using linear combinations of AdoCbl and HOCbl showed that a 1:1 (0.2 eq.: 0.2 eq.) ratio was able to account for the spectrum (Figure 2S, SI). This result is consistent with only 0.8 eq. of AdoCbl being used for complete inactivation. The spectrum for the small molecules observed at 2 min could not be not be recapitulated by any combination of AdoCbl and HOCbl and at a minimum requires the presence of a third species. While we have obtained a spectrum of this putative third species that appears to be a cobalt III species (data not shown), the length of time of the experiment and the concentration of the sample by lyophilization, make any discussion of its structure and whether it is the precursor to RTPR alkylated with a corrin at C_{419} (C419-S corrin), premature.

Identification and quantification of product(s) derived from the F_2CTP ribose ring

In the accompanying manuscript using 1 eq. of [5-^{3}H]-F_2CTP, the release of 0.7 eq. of cytosine was found to accompany RTPR inactivation when the reaction mixture was analyzed at 2 min, although the work up took several hours. Furthermore, studies with [1′-^{3}H]-F_2CTP under identical conditions, indicated that 0.47 eq. of sugar was covalently attached to RTPR and that ~0.2 eq. of F_2C was recovered. Thus, ~0.3 eq. of the nucleotide is unaccounted for. To find this missing material, inactivations were initially performed using [1′-^{3}H]-F_2CTP and the small molecules separated from RTPR by ultrafiltration (10 min at 14,000 × g at 4°C) at 2 min. The nucleotides were examined by ion-pairing reverse-phase HPLC. The HPLC trace showed new nucleotide products that eluted just prior to F_2CTP. These results suggested that there is a nucleotide that has dissociated from RTPR that can eliminate cytosine on a relatively slow timescale. If F_2CTP has been converted to a 3′-ketone as observed for other mechanism based inhibitors (see Scheme 1 in the accompanying manuscript), it should be possible to reduce it

with $NaBH_4$, trapping the product(s) before cytosine and inorganic tripolyphosphate are eliminated.

The inactivation reaction was thus carried out with [1′-^{3}H]-F_2CTP for 2 min and then reacted with $NaBH_4$ for 5 min. After the phosphates of the nucleotides were removed with alkaline phosphatase, the reaction mixture was analyzed by reverse-phase HPLC with diode array detection. Under these conditions, in a typical experiment, a small amount of material (<5%) eluted in the solvent front, 0.25 eq. of F_2C was recovered and a new, broad peak of radioactivity (0.28 eq.) was observed with retention time of 17–22 min and λ_{max} at 270 nm, consistent with cytosine-like nucleosides (Figure 2A). The new nucleosides (between the arrow in Figure 2A) were pooled and re-purified twice to give a single peak (Figure 2B) with 50% recovery. In each repurification, only the nucleoside with the shorter retention time was pooled. This peak elutes earlier than in the initial purification due to the use of a smaller injection loop (0.5 mL vs. 2 mL). There are several reasonable explanations for the heterogeneity of the trapped nucleosides. One explanation is that there was no effort to ensure removal of the borate esters resulting from the reduction process prior to the first chromatography. Repurification and lyophilization in the presence of the NH_4OAc buffer, however, could have catalyzed this hydrolysis and resulted in a more homogeneous sample. A second explanation is that the reduction with $NaBH_4$ of a ketone would produce diastereomers that are separable by HPLC.

The final product isolated by HPLC was analyzed by NMR spectroscopy and is shown in Figure 3A. The protons at 7.71 and 5.85 ppm are consistent with the H6 and H5 protons of cytosine, while the proton at 5.99 is consistent with the H1′ of a sugar of a nucleoside. An expansion of the sugar ring region from 3.5 to 4.5 ppm (Figure 3A′) showed that the chemical shifts and splitting patterns are similar, but not identical to those observed with cytosine arabinoside (*ara*-C) and cytidine (data not shown). This material has a different retention time from cytidine (12.6 min) and *ara*-C (17.4 min), but an ESI MS indicates a cytidine isomer. The results together suggest that the nucleoside is an isomer of cytidine differing in stereochemistry at one or more carbons. Selective purification of nucleoside (Figure 2) is likely to have removed other diastereomers. The trapped nucleoside leads to the surprising conclusion that not only have both fluorines been eliminated from the F_2CTP, but that an oxygen has been added!

To gain information about the precursor to this cytidine analog, the inactivation was repeated, using $NaBD_4$ in place of $NaBH_4$ in the quenching process. Our studies with many mechanism based inhibitors suggested that the radical trapped could be a cytidine derivative with a 3′-ketone and perhaps a radical at C2′ (**6**, Scheme 2).(3,27–31) This radical could rearrange to a 2′-keto, 3′ radical through a semidione radical intermediate. Reduction with $NaBD_4$ could then potentially give a mixture of cytidine analogs with ^{2}H at C-2′ and at C-3′. HPLC chromatography of the reaction mixture revealed that the major trapped nucleoside was similar to that observed by $NaBH_4$ trapping (Figure 2A). The second chromatography of this pooled material is shown in Figure 2C. The third repurification looked like Figure 2B. The material was further purified and characterized by NMR spectroscopy (Figure 3B with an expansion of the sugar region shown in Figure 3B′). The results of this analysis revealed yet another surprise. Greater than 99% [^{2}H] incorporation was observed at both the 2′ and 3′ positions of the nucleoside. The chemical shifts of this trapped material are the same as in the $NaBH_4$ trapped material. The signals, however, for the 2′ and 3′ hydrogens are absent, the signal for 1′ has collapsed to a singlet and the signal for the 4′ hydrogen has collapsed to a doublet of doublets.

This result requires that the direct precursor to reduction is not a monoketonucleotide as expected, but the 2′,3′-diketonucleotide. This compound would be unable to eliminate cytosine. Thus the observation of cytosine provides insight into the timing of formation of this material. In the cytosine quantification experiments, it was found that after dephosphorylation of the product mixtures, a process that takes several hours at 37°C, the only cytosine-containing

compounds were cytosine and F_2C. Thus to account for this product, the radical precursor must be oxidized under the $NaBH_4$quench conditions.

A model for the observed deuterium incorporation is illustrated in Scheme 2. Initial deprotonation of the hydroxyketone radical (**6**) would generate a semidione radical anion. (32) This compound might undergo reduction by hydride transfer from $NaBH_4$, giving rise **8**. Loss of an electron from **8**, perhaps to O_2 or a cobalamin species, would generate a second ketone, which could then be further reduced by $NaBH_4$ to **9**. Reduction of this new ketone would give the observed ^2H incorporation. The mechanism of the oxidation process is not known.

Preliminary studies using [1′-^{2}H]-F_2CTP and [3′-^{2}H]-F_2CTP and high field ENDOR to probe the structure of new radical species generated by the exchange coupled thiyl radical•cob(II) alamin: Evidence that this new species is nucleotide based

[1′-^{2}H]-F_2CTP and [3′-^{2}H]-F_2CTP were used to investigate the structure of the radical formed upon inactivation of RTPR using X-band (9 GHz) and D-band (130 GHz) EPR methods. Inactivation studies were carried out and the samples were quenched by hand at 20 or 30 s in an isopentane/liquid N_2 slurry. The radical observed with [1′-^{2}H]-F_2CTP and [3′-^{2}H]-F_2CTP was identical to the one we previously reported at 9 GHz (data not shown)(17). Similar analysis was carried out at high field (130 GHz). No differences were noted between the unlabeled inhibitor and the [3′-^{2}H] F_2CTP experiments. With [1′-^{2}H]-F_2CTP/RTPR, the spectrum was subtly different from the unlabeled inhibitor (Supporting Information, Figure 3S), however, it was unclear whether these differences resulted from deuteration or though interaction with minor radical species. High frequency ENDOR had a greater potential to show coupling between the deuteron and the radical. The results of these experiments are shown in Figure 4. The spectral regions in which deuteron and proton resonances are expected to be observed are displayed in Figure 4A and B, respectively. At magnetic fields used for D-band ENDOR, the Larmor frequencies of deuterium (31 MHz) and protium (199 MHz) are well separated and typically provide non-overlapping spectra. The results of an experiment using [1′-^{2}H]-F_2CTP are shown in Figure 4A and exhibit 8.6 MHz coupling of the radical to a deuteron. (Note: the quadrupole splitting expected for the deuteron (I = 1) is presumably too small to be resolved in the spectrum). The corresponding proton coupling in the radical derived from unlabeled F_2CTP is evident in Figure 4B (upper trace): the peaks at 169 and 226 MHz are split by an amount equal to ($\gamma H/\gamma D$) × 8.6 MHz, in which γH and γD are the proton and deuteron gyromagnetic ratios, respectively. This proton coupling is absent in the [1′-^{2}H]-F_2CTP sample (Figure 4B bottom). The relative narrowness of both the proton and deuteron peaks together with the insensitivity of the size of the coupling to the excitation position in the EPR spectrum (data not shown) suggest an approximately isotropic hyperfine coupling. In addition, no phosphorus or nitrogen ENDOR couplings were observed (data not shown). These results are consistent with a radical species that has significant unpaired electron spin density at the 2′-position. This unpaired spin density would be expected to couple to the 1′ deuteron/proton via a largely isotropic, β-hydrogen type mechanism.(33,34) These preliminary results provided the first direct evidence that the observed organic radical is indeed a nucleotide-based radical and provides support for a mechanism that produces a stable, 2′-radical.

DISCUSSION

A non-alkylative, pathway required for complete inactivation of RTPR by F_2CTP involves reaction of the enzyme with the AdoCbl ultimately resulting in the formation of a bond between the Co in the corrin and S of C_{419} that we have previously characterized.(17) Our studies examining the fate of AdoCbl in this paper, reveal that after 2 min, 0.25 eq. of cobalt III species co-elutes with RTPR and display a spectrum consistent with a corrin containing a Co-S bond

(compare Fig 1A with Fig. 1S). By 1 h, this species (Fig. 1B) has increased to 0.45 eq., with a corresponding decrease in corrin species in solution. The unidentified Co(III) species present in the small molecules at 2 min disappears by 1 h, suggesting it is converted into the Co-S adduct. Thus, 100% inactivation is associated with a tightly bound AdoCbl analog in the +3 oxidation state, that is slowly converted into the previously characterized Co-S adduct.

In addition to this tightly bound corrin associated with RTPR at 2 min, 0.25 eq. of a nucleotide derived from F_2CTP was trapped with $NaBH_4$ in which both fluorines were lost and a water molecule was added. As argued subsequently, our hypothesis is that this trapped nucleotide is derived from radical **4** in Scheme 1. While the identity of **4** has not been unambiguously established, the HFEPR/HFENDOR data presented, are consistent with a 3′ keto, 2′ oxoallylic radical species such as **4**. The largely isotropic 1′-^{1}H/^{2}H coupling of 57/8.6 MHz is in agreement with calculations published previously for such a radical species.(35) In addition, the splitting in the proton spectra of approximately 13 MHz (Figure 4B) is consistent with calculations for the proton at the 4′ position.(35) From the EPR data, there is no evidence for the presence of fluorine, consistent with **4**.

Our working hypothesis that accounts for the non-alkylative pathway and formation of **4** is shown in Scheme 1. Our previous RFQ EPR experiments during the inactivation of RTPR by F_2CTP, revealed that a thiyl radical exchange coupled to cob(II)alamin (1.4 radical eq.) was present within 20 ms, the first time point. This radical pair gave rise quantitatively to a new radical pair over 220 ms that is proposed to be **2**↔ **3** and cob(II)alamin (Scheme 1). Formation of **2**↔ **3** is proposed to occur, by loss of F^- without protonation by the proximal bottom-face cysteine, C_{119}. The loss of F^- and not HF, might result if the ribose ring of the nucleotide is too far removed from C_{119}, as suggested by the recent crystal structure of the *S cerevisiae* RNR.(36) Alternatively, F^- loss may simply be related to its leaving group ability being intermediate between hydroxide, which with the normal substrate must be protonated to leave at a reasonable rate, and chloride, which can be lost without protonation.(37) Radical **2**↔ **3**, the species we believe was detected at 220 ms by RFQ experiments, could then react with water at the **2′ C,** in a reaction that is the reversal of water elimination in the normal reaction (considered irreversible for the normal, non-fluorinated substrate). In the non-alkylative pathway, **3** could now eliminate the second F^-, generating **4**, the favored structure for the stable radical seen at 20 s.(17) This radical is structurally very similar to the stable glycoaldehyde radical detected when diol dehydratase is inactivated by glycoaldehyde.(32,38) The glycoaldehyde radical is reported to be stable for days at room temperature under anaerobic conditions. Radical **4** could dissociate from the active site and eventually decompose to eliminate cytosine or be trapped if $NaBH_4$ is present, prior to cytosine release. In the alkylative pathway (**3** to **5**, Scheme 1), we propose that protonation of F^- occurs by C_{119}, giving loss of HF. The resulting thiolate of C_{119}, could now attack the C2′ of the nucleotide to form the alkylated protein.

The model of inactivation of RTPR by F_2CTP is complex, but shares many common features with inactivation of the class Ia RNRs (*E. coli* and the two human RNRs) despite the differences in the cofactor requirement.(39–41) In each enzyme the inactivation is stoichiometric and involves multiple pathways: alkylation of an active site cysteine and destruction of the cofactor (AdoCbl or Y•). The alkylation is accompanied by a change in conformation of the RNR large subunit (α) that can be observed by SDS PAGE analysis if the sample is not boiled prior to loading on the gel. The conformational change results in an α that migrates more slowly than the unmodified α.(41) In both the case of the *E. coli* RNR and the *L. leichmannii* RNR, a new nucleotide radical is generated, resulting in the destruction of the cofactor.(41) In both cases we propose that the structure of the radical is the same, resulting from the loss of two fluorines and addition of a water molecule. The major distinction between F_2C nucleotides and previously studied 2′-substituted-2′-deoxynucleotides is the presence of the second leaving group. As with many fluorinated mechanism based inhibitors, the presence of the second

fluoride causes the reaction to be irreversible.(42) The similarities between the chemistry of the class I and II RNRs suggest that lessons learned from our studies on inactivation of the *L. leichmannii* RTPR, will likely be very informative about the mechanisms of inactivation of the class Ia RNRs by this clinically useful antitumor agent.

Supplementary Material

Refer to Web version on PubMed Central for supplementary material.

Abbreviations

RNR	ribonucleotide reductase
eq.	equivalent
Gemzar™	F_2C, 2′,2′-difluoro-2′-deoxycytidine
F_2CDP 2′	2′-difluoro-2′-deoxycytidine 5′-diphosphate
F_2CTP 2′	2′-difluoro-2′-deoxycytidine 5′-triphosphate
RTPR	ribonucleoside triphosphate reductase
AdoCbl	adenosylcobalamin
SA	specific activity
HOCbl	hydroxycobalamin
ara-C	arabino-cytidine
RFQ	rapid freeze-quench
GSCbl	glutathionine cobalamin
Y•	tyrosyl radical
α	ribonucleotide reductase large subunit

REFERENCES

1. Stubbe J, van der Donk WA. Ribonucleotide reductases: radical enzymes with suicidal tendencies. Chem. Biol 1995;2:793–801. [PubMed: 8807812]
2. Stubbe J, van der Donk WA. Protein radicals in enzyme catalysis. Chem. Rev 1998;98:705–762. [PubMed: 11848913]
3. Licht, S.; Stubbe, J. Mechanistic investigations of ribonucleotide reductases. In: Barton, SD.; Nakanishi, K.; Meth-Cohn, O.; Poulter, CD., editors. Comprehensive Natural Products Chemistry. New York: Elsevier Science; 1999. p. 163-203.
4. Eklund H, Uhlin U, Färnegårdh M, Logan DT, Nordlund P. Structure and function of the radical enzyme ribonucleotide reductase. Prog. Biophys. Mol. Biol 2001;77:177–268. [PubMed: 11796141]
5. Nordlund P, Reichard P. Ribonucleotide reductases. Annu. Rev. Biochem 2006;75:681–706. [PubMed: 16756507]
6. Hertel LW, Boder GB, Kroin JS, Rinzel SM, Poore GA, Todd GC, Grindley GB. Evaluation of the antitumor activity of gemcitabine (2',2'-difluoro-2'-deoxycytidine). Cancer Res 1990;51:6110–6117. [PubMed: 1718594]
7. Hertel, LW.; Kroin, JS.; Grossman, CS.; Grindey, GB.; Door, AF.; Storinolo, AMV.; Plunkett, W.; Gandhi, V.; Huang, P. Synthesis and biological activity of 2′,2′-difluorodeoxycytidine (gemcitabine). In: Ojima, I.; McCarthy, JR.; Welch, JT., editors. Biomedical Frontiers of Fluorine Chemistry. Washington, D. C: American Chemical Society; 1996.
8. Huang P, Chubb S, Hertel LW, Grindey GB, Plunkett W. Action of 2′,2′-difluorodeoxycytidine on DNA synthesis. Cancer Res 1991;51:6110–6117. [PubMed: 1718594]

9. Davidson JD, Ma L, Flagella M, Geeganage S, Gelbert LM, Slapak CA. An increase in the expression of ribonucleotide reductase large subunit 1 is associated with gemcitabine resistance in non-small cell lung cancer cell lines. Cancer Res 2004;64:3761–3766. [PubMed: 15172981]
10. Danesi R, Altavilla G, Giovannetti E, Rosell R. Pharmacogenetics of gemcitabine in non-small-cell lung cancer and other solid tumors. Pharmacogenetics 2009;10:69–80.
11. Rivera F, López-Tarruella S, Vega-Villegas ME, Salcedo M. Treatment of advanced pancreatic cancer: from gemcitabine single agent to combinations and targeted therapy. Cancer Treat. Rev 2009;35:335–339. [PubMed: 19131170]
12. Jordan A, Torrents E, Jeanthon C, Eliasson R, Hellman U, Wernstedt C, Barbé J, Gibert I, Reichard P. B_{12}-dependent ribonucleotide reductases from deeply rooted eubacteria are structurally related to the aerobic enzyme from *Escherichia coli*. Proc. Natl. Acad. Sci. U. S. A 1997;94:13487–13492. [PubMed: 9391052]
13. Booker S, Stubbe J. Cloning, sequencing and expression of the adenosylcobalamin-dependent ribonucleotide reductase from *Lactobacillus leichmannii*. Proc. Natl. Acad. Sci. U. S. A 1993;90:8352–8356. [PubMed: 8397403]
14. Sintchak MD, Arjara G, Kellogg BA, Stubbe J, Drennan CL. The crystal structure of class II ribonucleotide reductase reveals how an allosterically regulated monomer mimics a dimer. Nature Struct. Biol 2002;9:293–300. [PubMed: 11875520]
15. Larsson K-M, Jordan A, Eliasson R, Reichard P, Logan DT, Nordlund P. Structural mechanism of allosteric substrate specificity regulation in a ribonucleotide reductase. Nature Struct. Mol. Biol 2004;11:1142–1149. [PubMed: 15475969]
16. Lohman GJS, Stubbe J. Inactivation of *Lactobacillus leichmannii* ribonucleotide reductase by F_2CTP: covalent modification. submitted to Biochemistry. 2009
17. Silva DJ, Stubbe J, Samano V, Robins MJ. Gemcitabine 5′-triphosphate is a stoichiometric mechanism-based inhibitor of *Lactobacillus leichmannii* ribonucleoside triphosphate reductase: evidence for thiyl radical-mediated nucleotide radical formation. Biochemistry 1998;37:5528–5535. [PubMed: 9548936]
18. Stubbe J, Riggs-Gelasco P. Harnessing free radicals: formation and function of the tyrosyl radical in ribonucleotide reductase. Trends Biochem. Sci 1998;23:438–443. [PubMed: 9852763]
19. Bandarian V, Ludwig ML, Matthews RG. Factors modulating conformational equilibria in large modular proteins: A case study with cobalamin-dependent methionine synthase. Proc. Natl. Acad. Sci. U. S. A 2003;100:8156–8163. [PubMed: 12832615]
20. Krymov V, Gerfen GJ. Analysis of the tuning and operation of reflection resonator EPR spectrometers. J. Magn. Reson 2003;162:466–478. [PubMed: 12810032]
21. Ranguelova K, Girotto S, Gerfen GJ, Yu S, Suarez J, Metlitsky L, Magliozzo RS. Analysis of the tuning and operation of reflection resonator EPR spectrometers. J. Biol. Chem 2007;282:6255–6264. [PubMed: 17204474]
22. Burhaus O, Rohrer M, Plato M, Mobius K. A novel high-field/high frequency EPR and ENDOR spectrometer operating at 3 mm wavelength. Meas. Sci. Tech 1992;3:765–774.
23. Booker S, Licht S, Broderick J, Stubbe J. Coenzyme B_{12}-dependent ribonucleotide reductase: evidence for the participation of five cysteine residues in ribonucleotide reduction. Biochemistry 1994;33:12676–12685. [PubMed: 7918494]
24. Licht SS, Booker S, Stubbe J. Studies on the catalysis of carbon-cobalt bond homolysis by ribonucleoside triphosphate reductase: evidence for concerted carbon-cobalt bond homolysis and thiyl radical formation. Biochemistry 1999;38:1221–1233. [PubMed: 9930982]
25. Licht SS, Lawrence CC, Stubbe J. Thermodynamic and kinetic studies on carbon-cobalt bond homolysis by ribonucleoside triphosphate reductase: the importance of entropy in catalysis. Biochemistry 1999;38:1234–1242. [PubMed: 9930983]
26. Licht SS, Lawrence CC, Stubbe J. Class II ribonucleotide reductases catalyze carbon-cobalt bond reformation on every turnover. J. Am. Chem. Soc 1999;121:7463–7468.
27. Ator MA, Stubbe J. Mechanism of inactivation of *Escherichia coli* ribonucleotide reductase by 2′-chloro-2′-deoxyuridine 5′-diphosphate: evidence for generation of 2′-deoxy-3′-ketonucleotide via a net 1,2 hydrogen shift. Biochemistry 1985;24:7214–7221. [PubMed: 3910098]

28. Harris G, Ator M, Stubbe J. Mechanism of inactivation of *Escherichia coli* and *Lactobacillus leichmannii* ribonucleotide reductases by 2′-chloro-2′-deoxynucleotides: evidence for generation of 2-methylene-3(2*H*)-furanone. Biochemistry 1984;23:5214–5225. [PubMed: 6391538]
29. van der Donk WA, Stubbe J, Gerfen GG, Bellew BF, Griffin RG. EPR investigations of the inactivation of *E. coli* ribonucleotide reductase with 2′-azido-2′-deoxyuridine 5′-diphosphate: evidence for the involvement of the thiyl radical of C225-R1. J. Am. Chem. Soc 1995;117:8909–8916.
30. van der Donk WA, Yu G, Pérez L, Sanchez RJ, Stubbe J. Detection of a new substrate-derived radical during inactivation of ribonucleotide reductase from *Escherichia coli* by gemcitabine 5′-diphosphate. Biochemistry 1998;37:6419–6426. [PubMed: 9572859]
31. Gerfen GG, van der Donk WA, Yu G, McCarthy JR, Jarvi ET, Matthews DP, Farrar C, Griffin RG, Stubbe J. Characterization of a substrate-derived radical detected during the inactivation of ribonucleotide reductase from *Escherichia coli* by 2′-fluoromethylene-2′-deoxycytidine 5′-diphosphate. J. Am. Chem. Soc 1998;120:3823–3835.
32. Sandala GM, Smith DM, Coote ML, Golding BT, Radom L. Insights into the hydrogen-abstraction reactions of diol dehydratase: relevance to the catalytic mechanism and suicide inactivation. J. Am. Chem. Soc 2006;128:3433–3444. [PubMed: 16522124]
33. Heller C, McConnell HM. Radiation Damage in Organic Crystals. II. Electron Spin Resonance of (CO2H)CH2CH(CO2H) in beta-Succinic Acid. J. Chem. Phys 1960;32:1535–1539.
34. Derbyshire W. The coupling between an unpaired electron spin and a proton two bonds away. Mol. Phys 1962;5:225–231.
35. Zipse H, Artin E, Wnuk S, Lohman GJ, Martino D, Griffin RG, Kacprzak S, Kaupp M, Hoffman B, Bennati M, Stubbe J, Lees N. Structure of the nucleotide radical formed during reaction of CDP/TTP with the E441Q-α2β2 of *E. Coli* ribonucleotide reductase. J. Am. Chem. Soc 2009;131:200–211. [PubMed: 19128178]
36. Xu H, Faber C, Uchiki T, Racca J, Dealwis C. Structures of eukaryotic ribonucleotide reductase I define gemcitabine diphosphate binding and subunit assembly. Proc. Natl. Acad. Sci. U. S. A 2006;103:4028–4033. [PubMed: 16537480]
37. Harris G, Ashley GW, Robins MJ, Tolman RL, Stubbe J. 2′-Deoxy-2′-halonucleotides as alternate substrates and mechanism-based inactivators of *Lactobacillus leichmannii* ribonucleotide reductase. Biochemistry 1987;26:1895–1902. [PubMed: 3297135]
38. Abend A, Bandarian V, Reed GH, Frey PA. Identification of *cis*-ethanesemidione as the organic radical derived from glycolaldehyde in the suicide inactivation of dioldehydrase and of ethanolamine ammonia-lyase. Biochemistry 2000;39:6250–6257. [PubMed: 10821701]
39. Wang J, Lohman GJ, Stubbe J. Enhanced subunit interactions with gemcitabine-5'-diphosphate inhibit ribonucleotide reductases. Proc. Nat. Acad. Sci. USA 2007;104:14324–14329. [PubMed: 17726094]
40. Wang J, Lohman GJ, Stubbe J. Mechanism of inactivation of human ribonucleotide reductase with p53R2 by gemcitabine-5'-diphosphate. Biochemistry in press. 2009
41. Artin E, Wang J, Lohman GJS, Yu G, Griffin RG, Barr G, Stubbe J. Insight into the mechanism of inactivation of ribonucleotide reductase by gemcitabine 5'-diphosphate in the presence and absence of reductant. Biochemistry in press. 2009
42. Walsh CT. Fluorinated substrate analogs: routes of metabolism and selective toxicity. Adv. Enzymol. Relat. Areas. Mol. Biol 1983;55:197–289. [PubMed: 6353888]

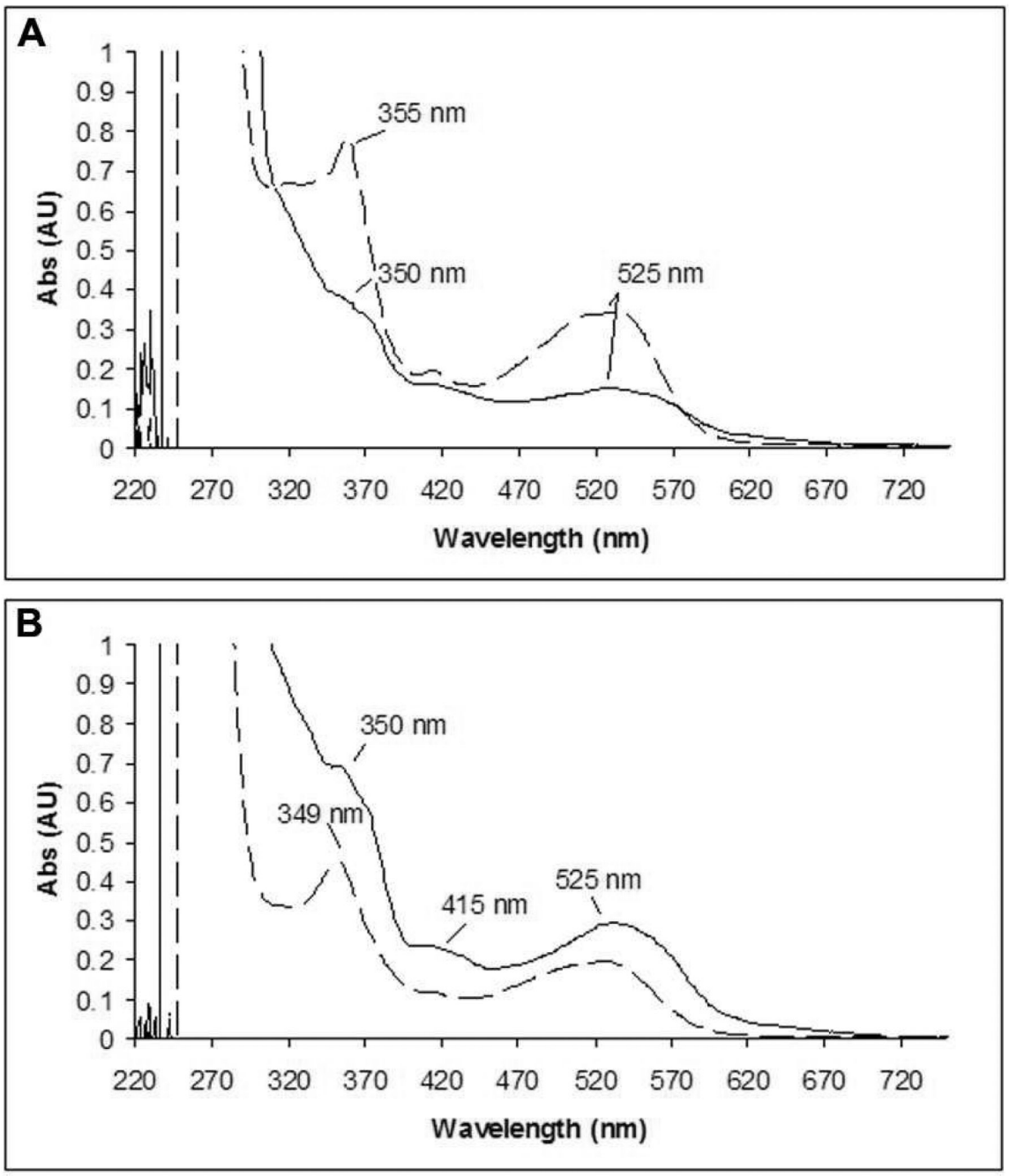

FIGURE 1.

UV-vis spectra of AdoCbl analog(s) bound to RTPR (solid line) and in solution (dashed line) subsequent to Sephadex G50 chromatography of RTPR inactivated by F_2CTP in the presence of 1 eq. of AdoCbl. (A) after 2 min. (B) after 1 h.

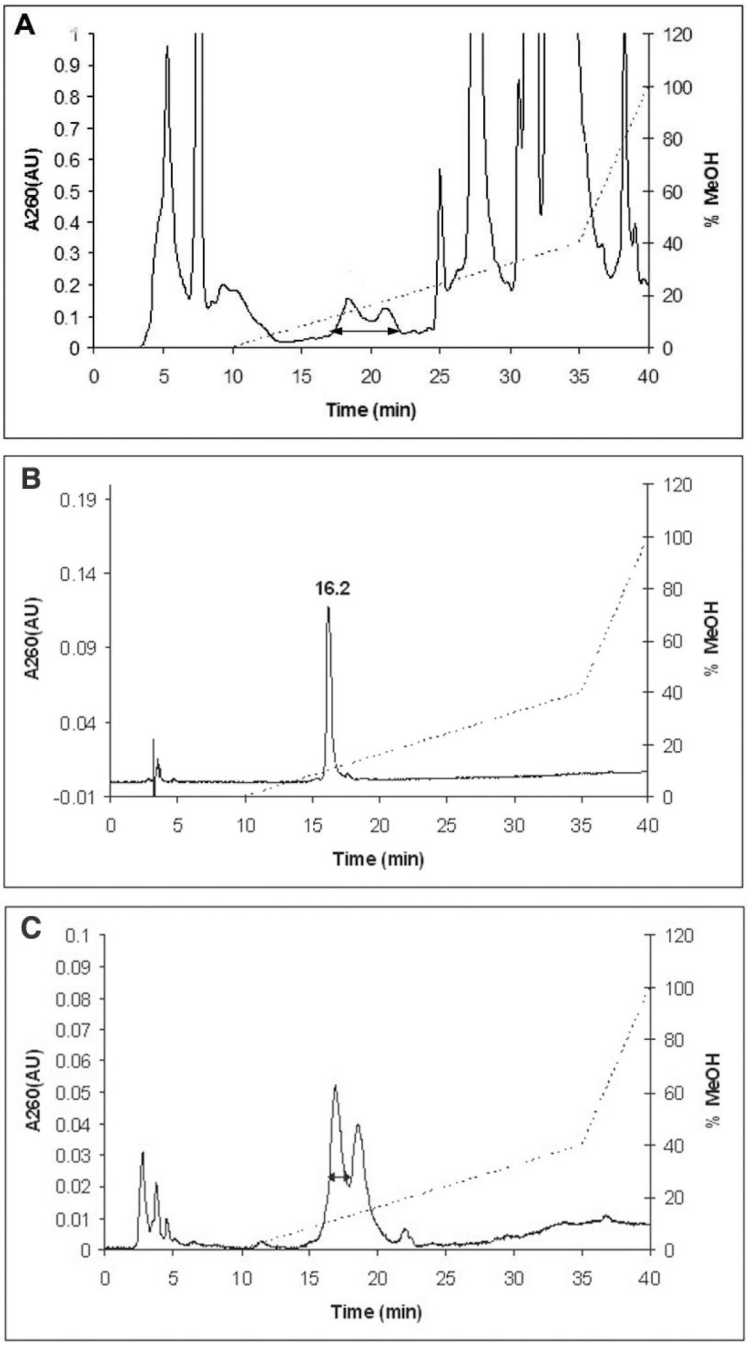

FIGURE 2.

Reverse-phase HPLC of small molecules from RTPR inactivated by F_2CTP, treated with $NaBH_4$, and dephosphorylated with alkaline phosphatase. A(260) (solid line), HPLC gradient (·····): Buffer A, 10 mM NH_4OAc, pH 6.8; Buffer B: methanol. The double headed arrow indicates the region pooled in each step. (A) Initial purification: the material eluting from 17–22 min was collected. (B) Elution of final purified product after two further repurifications under the same conditions. (C) Reverse-phase HPLC of small molecules from RTPR inactivated with F_2CTP, treated with $NaBD_4$, and dephosphorylated with alkaline phosphatase. This is the second step in the three step purification.

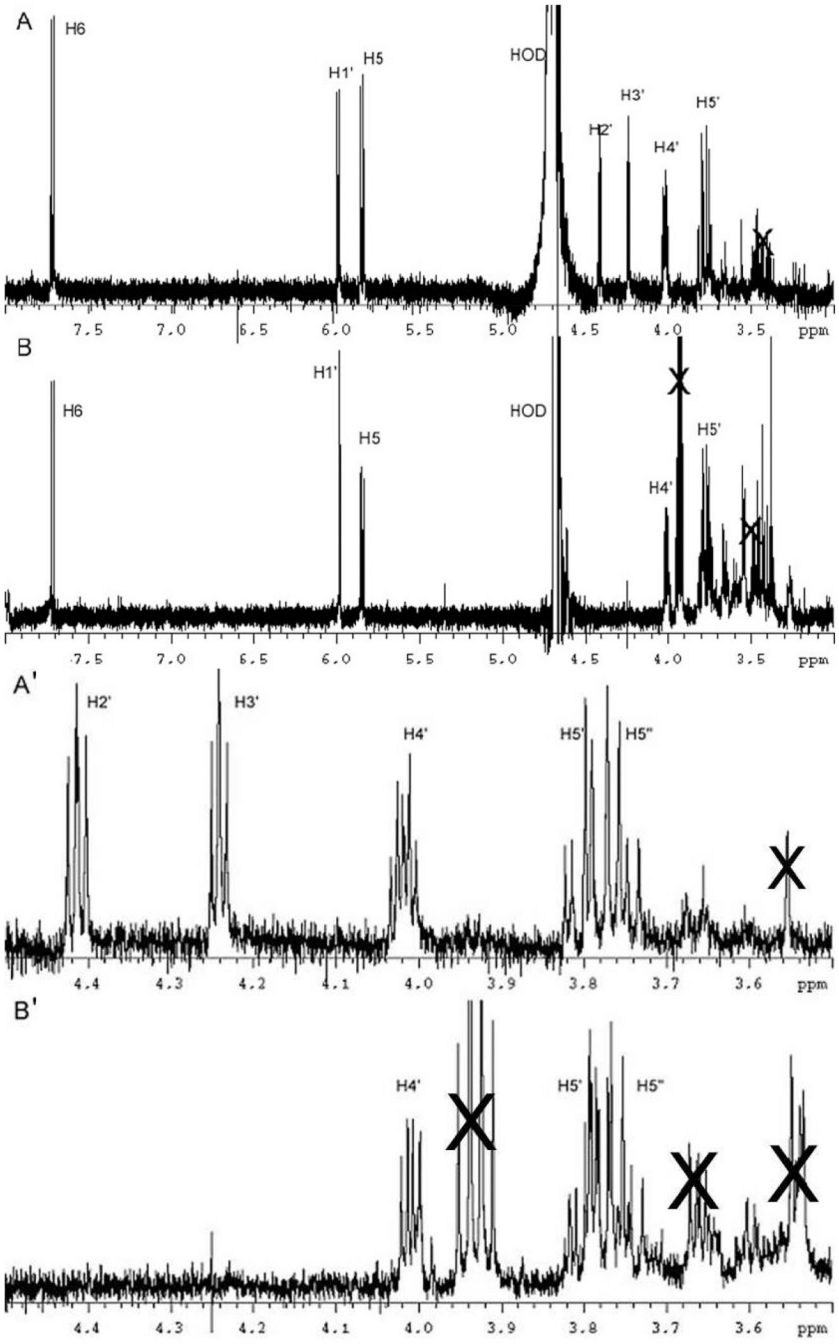

FIGURE 3.

Comparison of ^{1}H-NMR (500 MHz, D_2O) spectra of new products isolated from the $NaBH_4$ (NaB_2H_4) quench of RTPR inactivated with F_2CTP. (A) Product from $NaBH_4$ quench; (B) product from NaB_2H_4 quench. (A′ and B′ are expansions of A and B in the region from 3.5 to 4.5 ppm). The nucleoside proton resonances are labeled. Several impurity peaks can be seen; these are marked with X. Further, the H5–H5′ region in B appears to overlap with an impurity peak.

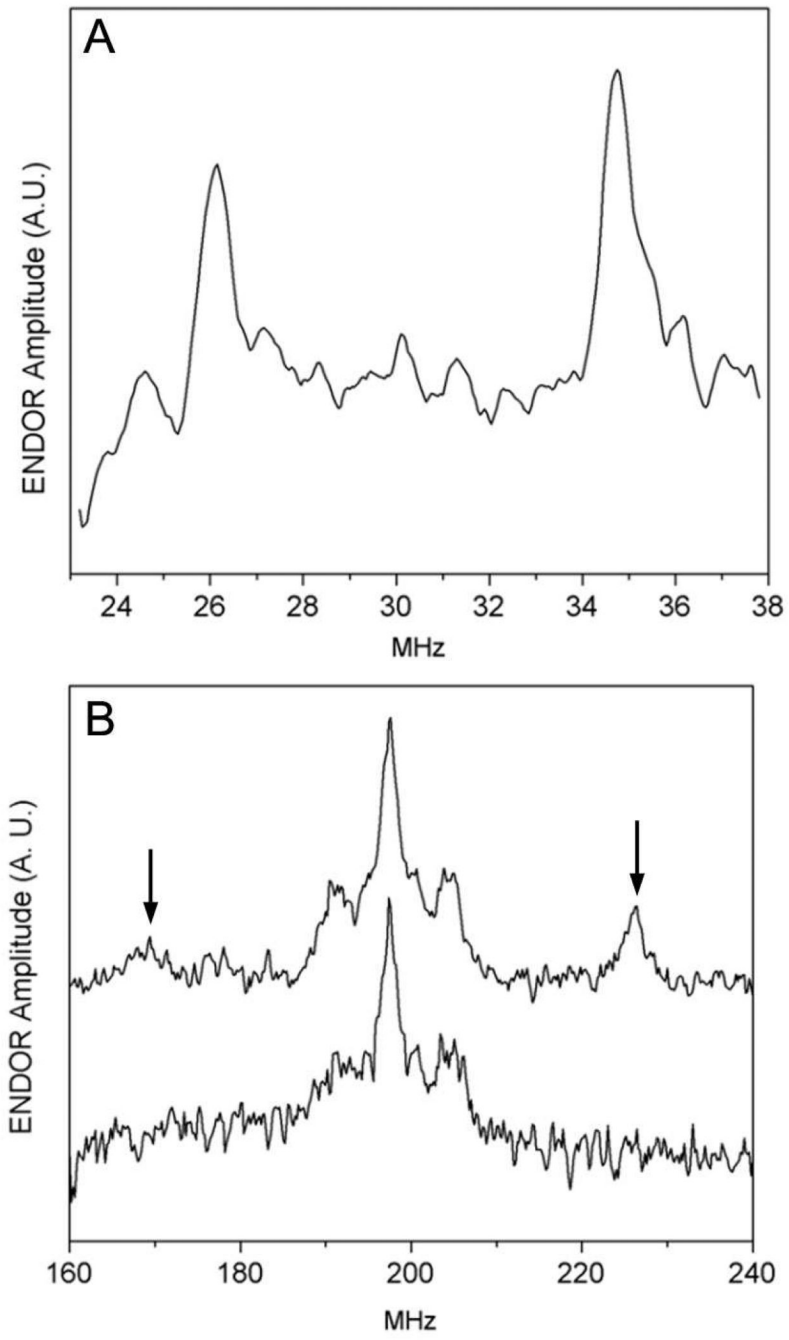

FIGURE 4.

High Frequency (130 GHz) Davies ENDOR of F_2CTP reacted with RTPR for 30 s. (A) Deuterium ENDOR of [1′-^{2}H]-F_2CTP reaction. Temperature 7 K; 8000 averages per point; pulse widths 80 ns, 40 ns, 80 ns; RF pulse width 20 μs, tau 200 ns; Rep rate 100 Hz (B) Proton ENDOR. Temperature 7 K; pulse widths 70 ns, 35ns 70ns ; RF pulse width 6.8 μs; tau 200 ns; Rep rate 100 Hz Upper trace: RTPR reacted with [1′-^{1}H]-F_2CTP, 800 averages per point. The peaks at 169 and 226 MHz are indicated. Lower Trace: RTPR reacted with [1′-^{2}H]-F_2CTP, 4500 averages per point

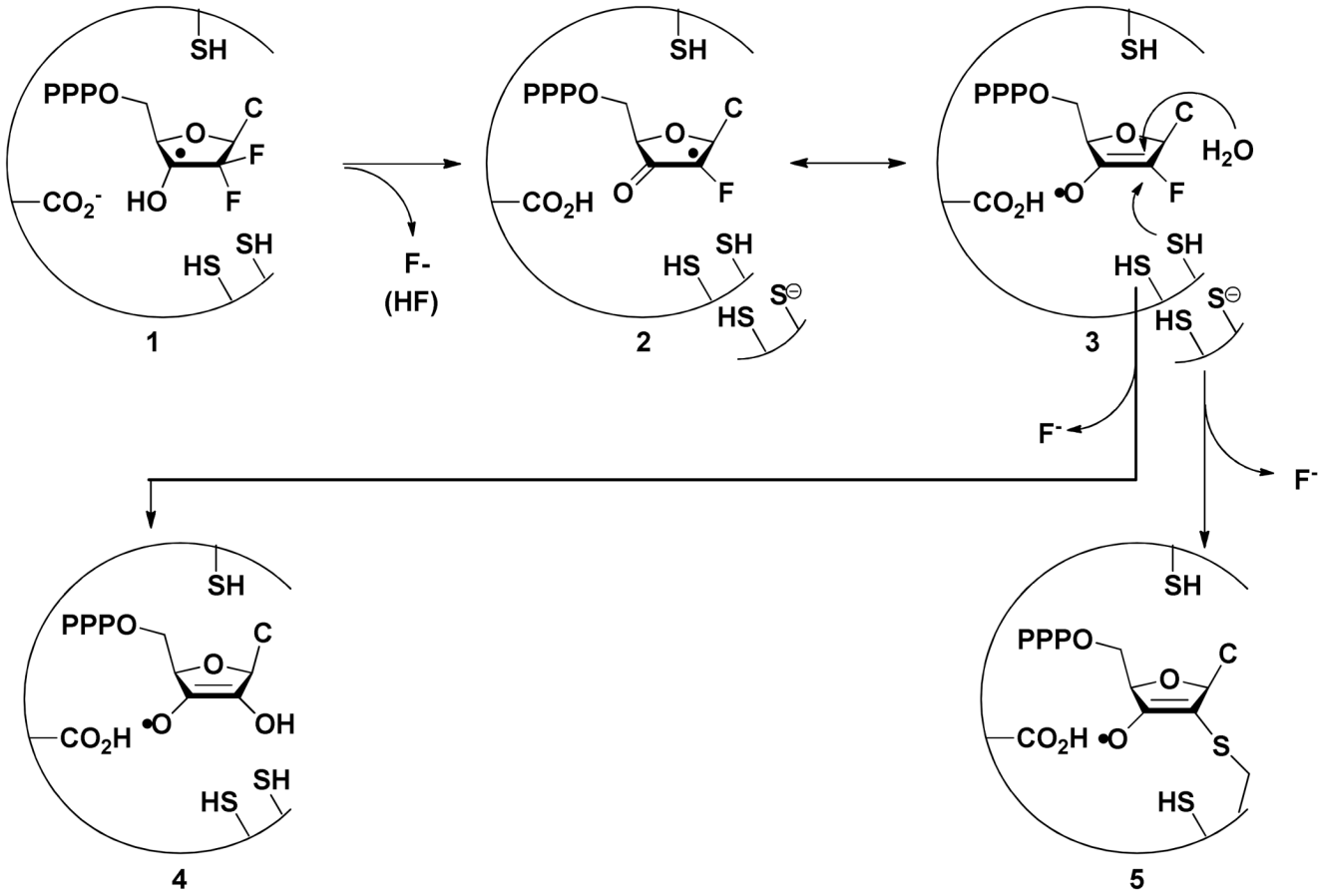

SCHEME 1.

Proposed model for the mechanism of inactivation by RTPR by F_2CTP by the non-alkylative and alkylative pathways.

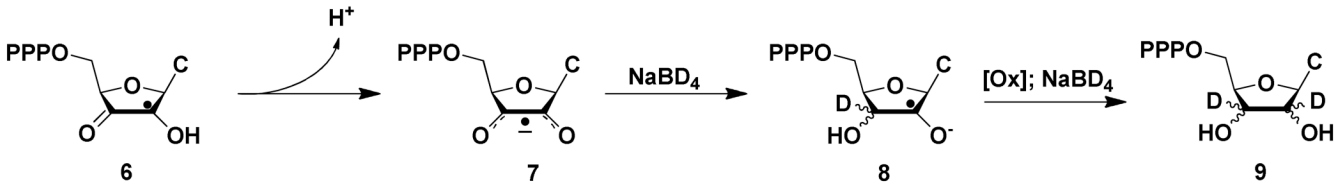

SCHEME 2.

Proposed mechanism for deuterium incorporation into the nucleotide trapped by NaB_2H_4 subsequent to the inactivation of RTPR by F_2CTP.